Energy Norm A Posteriori Error Estimation for Mixed Discontinuous Galerkin Approximations of the Stokes Problem

P. Houston*, D. Schötzau† and Th. Wihler

Research Report No. 2003-09
August 2003

Seminar für Angewandte Mathematik
Eidgenössische Technische Hochschule
CH-8092 Zürich
Switzerland

*Funded by the EPSRC (Grant GR/R76615). Department of Mathematics and Computer Science, University of Leicester, Leicester LE1 7RH, UK

†Partially supported by the Swiss NSF (Project 21-068126.02). Department of Mathematics, University of Basel, Rheinsprung 21, 4051 Basel, Switzerland

Energy Norm A Posteriori Error Estimation for Mixed Discontinuous Galerkin Approximations of the Stokes Problem

P. Houston*, D. Schötzau† and Th. Wihler

Seminar für Angewandte Mathematik
Eidgenössische Technische Hochschule
CH-8092 Zürich
Switzerland

Research Report No. 2003-09 August 2003

Abstract

In this paper, we develop the a posteriori error estimation of mixed discontinuous Galerkin finite element approximations of the Stokes problem. In particular, computable upper bounds on the error, measured in terms of a natural (mesh–dependent) energy norm, are derived. The proof of the a posteriori error bound is based on rewriting the underlying method in a non-consistent form by introducing appropriate lifting operators, and employing a decomposition result for the discontinuous spaces. A series of numerical experiments highlighting the performance of the proposed a posteriori error estimator on adaptively refined meshes are presented.

Keywords: Discontinuous Galerkin methods, A posteriori error estimation, Stokes problem.

*Funded by the EPSRC (Grant GR/R76615). Department of Mathematics and Computer Science, University of Leicester, Leicester LE1 7RH, UK

†Partially supported by the Swiss NSF (Project 21-068126.02). Department of Mathematics, University of Basel, Rheinsprung 21, 4051 Basel, Switzerland

1. Introduction

In recent years, several authors have been concerned with the development of mixed discontinuous Galerkin (DG, for short) methods for the numerical approximation of incompressible fluid flow problems. We mention here the works of Baker *et al.* [2] and Karakashian and Jureidini [15] who studied piecewise solenoidal discontinuous Galerkin methods for the Stokes and Navier-Stokes equations. Later, Cockburn *et al.* [6, 7] proposed and analyzed local discontinuous Galerkin discretizations for Stokes and Oseen flow. Finally, Hansbo and Larson [12], Toselli [20] and Girault *et al.* [11] employed mixed interior penalty methods for the approximation of saddle point problems arising in linear elasticity and fluid flow. The recent work of Toselli [20], Schötzau *et al.* [18] and Schötzau and Wihler [19] has been devoted to the extension of mixed DG methods from the h–version to the hp-version of the finite element method. The key advantages of discontinuous Galerkin approaches in comparison with standard conforming finite element methods lie in their robustness and stability in transport-dominated regimes, their flexibility in the mesh-design, and their freedom in the choice of velocity-pressure space pairs without the need for extensive stabilization.

While an extensive body of literature is available with a priori error analyses for discontinuous Galerkin discretizations applied to elliptic problems, there are considerably fewer papers that are concerned with a posteriori error estimation for such approaches. We mention here the recent work by Becker *et al.* [3, 4] and Karakashian and Pascal [16], where energy norm error estimators are derived for diffusion problems, as well as the article by Houston *et al.* [14], where computable upper bounds on the energy norm of the error in the mixed DG approximation to the time–harmonic Maxwell operator were established.

In this paper, we initiate the development of the a posteriori error estimation and adaptive mesh design for mixed discontinuous Galerkin approximations of the Stokes problem for incompressible fluid flow. In particular, computable upper bounds on the error, measured in terms of a natural (mesh–dependent) DG energy norm, will be derived. In contrast to the approach of Becker *et al.* [4] and Houston *et al.* [14], which is based on employing a suitable Helmholtz decomposition of the error, together with the underlying conservation properties of DG methods, here we present a new technique to derive a posteriori error bounds. Indeed, the analysis presented in this article is based on rewriting the method in a non-consistent manner using lifting operators in the spirit of Arnold *et al.* [1], Perugia and Schötzau [17] and Schötzau *et al.* [18], and employing the decomposition result for discontinuous spaces from Houston *et al.* [13]; the proof of this result is based on a crucial approximation property from Karakashian and Pascal [16, Section 2]. The performance of the proposed error bound within an adaptive mesh refinement procedure will be demonstrated for problems with both smooth and singular analytical solutions. In particular, the results show that the error estimator is asymptotically exact on non-uniform adaptively refined meshes.

The outline of the paper is as follows. In Section 2, we introduce a mixed discontinuous Galerkin method for the Stokes problem. In Section 3, our a posteriori error bound is presented and discussed. The derivation of this result can be found in Section 4. In Section 5, we present a series of numerical experiments to highlight the performance of the proposed error estimator within an automatic mesh refinement algorithm. Finally, in Section 6 we summarize the work presented in this paper and draw some conclusions.

2. Mixed DG Approximation of Stokes Flow

In this section, we introduce a mixed discontinuous Galerkin method for the discretization of the Stokes problem.

2.1. Function Spaces

We begin by defining the function spaces that will be used throughout the paper. Given a bounded domain D in $\mathbb{R}^d$, $d \geq 1$, we write $H^t(D)$ to denote the usual Sobolev space of real-valued functions with norm $\|\cdot\|_{t,D}$, $t \geq 0$. In the case $t = 0$, we set $L^2(D) = H^0(D)$. We define $H^1_0(D)$ to be the subspace of functions in $H^1(D)$ with zero trace on ∂D. In addition, we set $L^2_0(D) = \{q \in L^2(D) : \int_D q \, d\mathbf{x} = 0\}$. For a function space $X(D)$, let $X(D)^d$ and $X(D)^{d\times d}$ denote the spaces of vector and tensor fields whose components belong to $X(D)$, respectively. These spaces are equipped with the usual product norms which, for simplicity, are denoted in the same way as the norm in $X(D)$. For vectors $\mathbf{v}, \mathbf{w} \in \mathbb{R}^d$, and matrices $\underline{\sigma}, \underline{\tau} \in \mathbb{R}^{d\times d}$, we use the standard notation $(\nabla \mathbf{v})_{ij} = \partial_j v_i$, $(\nabla \cdot \underline{\sigma})_i = \sum_{j=1}^d \partial_j \sigma_{ij}$, and $\underline{\sigma} : \underline{\tau} = \sum_{i,j=1}^d \sigma_{ij}\tau_{ij}$. We denote by $\mathbf{v} \otimes \mathbf{w}$ the matrix whose ij-th entry is $v_i w_j$. Note that the following identity holds: $\mathbf{v} \cdot \underline{\sigma} \cdot \mathbf{w} = \sum_{i,j=1}^d v_i \sigma_{ij} w_j = \underline{\sigma} : (\mathbf{v} \otimes \mathbf{w})$.

2.2. The Stokes Problem

Given a bounded Lipschitz polygon $\Omega \subset \mathbb{R}^2$ with boundary $\Gamma = \partial\Omega$, we consider the Stokes problem: find the velocity field $\mathbf{u}$ and the pressure p such that

$$\begin{aligned} -\nu\Delta\mathbf{u} + \nabla p &= \mathbf{f} && \text{in } \Omega, && \text{(1a)}\\ \nabla\cdot\mathbf{u} &= 0 && \text{in } \Omega, && \text{(1b)}\\ \mathbf{u} &= \mathbf{0} && \text{on } \Gamma. && \text{(1c)} \end{aligned}$$

Here, $\mathbf{f} \in L^2(\Omega)^2$ is a given source term. The standard variational form of the Stokes problem reads: find $(\mathbf{u}, p) \in H_0^1(\Omega)^2 \times L_0^2(\Omega)$ such that

$$\begin{cases} \int_\Omega \nu\nabla\mathbf{u} : \nabla\mathbf{v}\, d\mathbf{x} \;-\; \int_\Omega p\nabla\cdot\mathbf{v}\, d\mathbf{x} \;=\; \int_\Omega \mathbf{f}\cdot\mathbf{v}\, d\mathbf{x},\\ \int_\Omega q\nabla\cdot\mathbf{u}\, d\mathbf{x} \;=\; 0 \end{cases}$$

for all $(\mathbf{v}, q) \in H_0^1(\Omega)^2 \times L_0^2(\Omega)$. Due to the continuous inf-sup condition

$$\inf_{0\neq q\in L_0^2(\Omega)} \sup_{0\neq\mathbf{v}\in H_0^1(\Omega)^2} \frac{-\int_\Omega q\nabla\cdot\mathbf{v}\, d\mathbf{x}}{\|\nabla\mathbf{v}\|_{0,\Omega}\|q\|_{0,\Omega}} \geq \kappa > 0, \tag{2}$$

where κ is the inf-sup constant, depending only on Ω, the variational formulation above is well-posed and has a unique solution $(\mathbf{u}, p) \in H_0^1(\Omega)^2 \times L_0^2(\Omega)$; see Girault and Raviart [10] or Brezzi and Fortin [5] for details.

The regularity results in Dauge [8] show that, under the foregoing assumptions, the solution $(\mathbf{u}, p)$ of the Stokes problem belongs to $H^{1+\varepsilon}(\Omega)^2 \times H^\varepsilon(\Omega)$ with a regularity exponent $\varepsilon > 0$. The maximal value of ε only depends on the opening angles at the corners of the domain. In particular, for a convex domain, we have $\varepsilon = 1$.

2.3. Meshes and Traces

Throughout, we assume that the domain Ω can be subdivided into shape-regular affine meshes $\mathcal{T}_h$ consisting of parallelograms $\{K\}$. For each $K \in \mathcal{T}_h$, we denote by $\mathbf{n}_K$ the unit outward normal vector on the boundary ∂K, and by h_K the elemental diameter. As usual, we define the mesh size by $h = \max_{K\in\mathcal{T}_h} h_K$.

An interior edge of $\mathcal{T}_h$ is the (non-empty) one-dimensional interior of $\partial K^+ \cap \partial K^-$, where K^+ and K^- are two adjacent elements of $\mathcal{T}_h$. Similarly, a boundary edge of $\mathcal{T}_h$ is the (non-empty) one-dimensional interior of $\partial K \cap \Gamma$ which consists of entire edges of ∂K. We denote by $\mathcal{E}_\mathcal{I}$ the union of all interior edges, by $\mathcal{E}_\mathcal{D}$ the union of all boundary edges, and set $\mathcal{E} = \mathcal{E}_\mathcal{I} \cup \mathcal{E}_\mathcal{D}$. We allow for irregular meshes, but suppose that the intersection between neighboring elements is either a common vertex or a common edge of at least one of the two elements. This implies that the local mesh sizes are of bounded variation, that is, there is a positive constant C such that $Ch_K \le h_{K'} \le C^{-1}h_K$, whenever K and K' share a common edge.

Next, we define the trace operators that are needed for the DG method. To this end, let K^+ and K^- be two adjacent elements of $\mathcal{T}_h$, and $\mathbf{x}$ an arbitrary point on the interior edge $e = \partial K^+ \cap \partial K^- \subset \mathcal{E}_{\mathcal{I}}$. Furthermore, let q, $\mathbf{v}$, and $\underline{\tau}$ be scalar-, vector-, and matrix-valued functions, respectively, that are smooth inside each element $K^\pm$. By $(q^\pm, \mathbf{v}^\pm, \underline{\tau}^\pm)$, we denote the traces of $(q, \mathbf{v}, \underline{\tau})$ on e taken from within the interior of $K^\pm$, respectively. Then, we introduce the following averages at $\mathbf{x} \in e$,

$$\{\!\{q\}\!\} = (q^+ + q^-)/2, \qquad \{\!\{\mathbf{v}\}\!\} = (\mathbf{v}^+ + \mathbf{v}^-)/2, \qquad \{\!\{\underline{\tau}\}\!\} = (\underline{\tau}^+ + \underline{\tau}^-)/2.$$

Similarly, the jumps at $\mathbf{x} \in e$ are given by

$$\begin{array}{ll} [\![q]\!] = q^+\,\mathbf{n}_{K^+} + q^-\,\mathbf{n}_{K^-}, & [\![\mathbf{v}]\!] = \mathbf{v}^+ \cdot \mathbf{n}_{K^+} + \mathbf{v}^- \cdot \mathbf{n}_{K^-}, \\ \underline{[\![\mathbf{v}]\!]} = \mathbf{v}^+ \otimes \mathbf{n}_{K^+} + \mathbf{v}^- \otimes \mathbf{n}_{K^-}, & [\![\underline{\tau}]\!] = \underline{\tau}^+\mathbf{n}_{K^+} + \underline{\tau}^-\mathbf{n}_{K^-}. \end{array}$$

On boundary edges $e \subset \mathcal{E}_{\mathcal{D}}$, we set $\{\!\{q\}\!\} = q$, $\{\!\{\mathbf{v}\}\!\} = \mathbf{v}$, $\{\!\{\underline{\tau}\}\!\} = \underline{\tau}$, as well as $[\![q]\!] = q\mathbf{n}$, $[\![\mathbf{v}]\!] = \mathbf{v} \cdot \mathbf{n}$, $\underline{[\![\mathbf{v}]\!]} = \mathbf{v} \otimes \mathbf{n}$, and $[\![\underline{\tau}]\!] = \underline{\tau}\mathbf{n}$. Here, $\mathbf{n}$ is the unit outward normal vector to the boundary Γ.

2.4. Discontinuous Galerkin Discretization

Given a mesh $\mathcal{T}_h$ and a polynomial degree $k \ge 1$, we approximate the Stokes problem by finite element functions $(\mathbf{u}_h, p_h) \in \mathbf{V}_h \times Q_h$, where

$$\begin{array}{rcl} \mathbf{V}_h &=& \{\, \mathbf{v} \in L^2(\Omega)^2 : \mathbf{v}|_K \in \mathcal{Q}^k(K)^2,\ K \in \mathcal{T}_h \,\}, \\ Q_h &=& \{\, q \in L^2_0(\Omega) : q|_K \in \mathcal{Q}^{k-1}(K),\ K \in \mathcal{T}_h \,\}. \end{array}$$

Here, $\mathcal{Q}^k(K)$ denotes the space of tensor product polynomials on K of degree k in each coordinate direction.

We consider the following discontinuous Galerkin approximation of the Stokes problem: find $(\mathbf{u}_h, p_h) \in \mathbf{V}_h \times Q_h$ such that

$$\left\{ \begin{array}{rcl} A_h(\mathbf{u}_h, \mathbf{v}) \;+\; B_h(\mathbf{v}, p_h) &=& \int_\Omega \mathbf{f} \cdot \mathbf{v}\, d\mathbf{x}, \\ -B_h(\mathbf{u}_h, q) &=& 0 \end{array} \right. \tag{3}$$

for all $(\mathbf{v}, q) \in \mathbf{V}_h \times Q_h$. The bilinear forms A_h and B_h are defined, respectively, by

$$A_h(\mathbf{u}, \mathbf{v}) \;=\; \nu \int_\Omega \nabla_h \mathbf{u} : \nabla_h \mathbf{v}\, d\mathbf{x} - \int_{\mathcal{E}} (\{\!\{\nu \nabla_h \mathbf{v}\}\!\} : \underline{[\![\mathbf{u}]\!]} + \{\!\{\nu \nabla_h \mathbf{u}\}\!\} : \underline{[\![\mathbf{v}]\!]})ds$$

$$
\begin{aligned}
&\quad +\nu \int_{\mathcal{E}} \mathtt{c}\underline{[\![\mathbf{u}]\!]} : \underline{[\![\mathbf{v}]\!]}\, ds, \\
B_h(\mathbf{v}, q) &= -\int_{\Omega} q\, \nabla_h \cdot \mathbf{v}\, d\mathbf{x} + \int_{\mathcal{E}} \{\!\{q\}\!\} [\![\mathbf{v}]\!]\, ds.
\end{aligned}
$$

Here, ∇_h denotes the discrete nabla operator that is taken elementwise. The function $\mathtt{c} \in L^\infty(\mathcal{E})$ is the so-called interior penalty function which is chosen as follows: writing $\mathtt{h} \in L^\infty(\mathcal{E})$ to denote the auxiliary mesh function defined by

$$
\mathtt{h}(\mathbf{x}) = \begin{cases} \min\{h_K, h_{K'}\}, & \mathbf{x} \in e = \partial K \cap \partial K' \subset \mathcal{E}_{\mathcal{I}}, \\ h_K, & \mathbf{x} \in e = \partial K \cap \partial \Omega \subset \mathcal{E}_{\mathcal{D}}, \end{cases}
$$

we set

$$
\mathtt{c} = \gamma \mathtt{h}^{-1}, \tag{4}
$$

with a parameter $\gamma > 0$ that is independent of the mesh size. To ensure coercivity of the underlying DG form A_h, the parameter γ must be chosen sufficiently large; see Arnold *at al.* [1] and the references therein.

It was recently shown that the mixed method defined in (3) satisfies a discrete inf-sup condition, and is thereby well-posed; for details, see Hansbo and Larson [12], Toselli [20], Schötzau *et al.* [18] and the references cited therein. Consequently, for (piecewise) smooth analytical Stokes solutions $(\mathbf{u}, p)$, the approximations $(\mathbf{u}_h, p_h)$ obtained from (3) satisfy a priori error bounds that are optimal in the mesh size and almost optimal in the polynomial degree. Extensions of these a priori results to Stokes solutions $(\mathbf{u}, p)$ with regularity below $H^2(\Omega)^2 \times H^1(\Omega)$ can be found in Schötzau and Wihler [19]; see also Wihler *et al.* [22] for closely related bounds for diffusion problems in non-smooth domains.

REMARK 2.1. *The discontinuous Galerkin form A_h in (3) is also referred to as the interior penalty form. Several other DG forms are available for the discretization of the Laplacian; see Arnold* et al. *[1] for a discussion and unifying approach of several DG methods for diffusion problems.*

We further point out that our mixed approximation in (3) is based on so-called mixed-order *elements (or $(\mathcal{Q}^k)^2 - \mathcal{Q}^{k-1}$ elements), where the approximation degree for the pressure is of one order lower than for the velocity. In view of the approximation properties, this pair is optimally matched. However, by introducing suitable pressure stabilization terms, it is also possible to employ* equal-order *elements (or $(\mathcal{Q}^k)^2 - \mathcal{Q}^k$ elements) with the same approximation degree for the velocity and the pressure; see the LDG approaches in Cockburn* et al. *[6, 7] for details.*

REMARK 2.2. *In the case of inhomogeneous Dirichlet boundary conditions* $\mathbf{u} = \mathbf{g}$ *on* Γ*, with a datum* $\mathbf{g}$ *satisfying the compatibility condition* $\int_\Gamma \mathbf{g}\cdot\mathbf{n}\,ds = 0$*, the functional on the right-hand side of the first equation in (3) must be replaced by*

$$F_h(\mathbf{v}) = \int_\Omega \mathbf{f}\cdot\mathbf{v}\,d\mathbf{x} - \int_{\mathcal{E}_\mathcal{D}} (\mathbf{g}\otimes\mathbf{n}) : \nabla_h \mathbf{v}\,ds + \int_{\mathcal{E}_\mathcal{D}} \mathtt{c}\mathbf{g}\cdot\mathbf{v}\,ds.$$

Additionally, the right-hand side of the second equation in (3) is set equal to

$$G_h(q) = -\int_{\mathcal{E}_\mathcal{D}} q\,\mathbf{g}\cdot\mathbf{n}\,ds.$$

3. A Posteriori Error Estimation

In this section we present and discuss an a posteriori estimator for the error measured in terms of the energy norm $\|\!|\cdot|\!\|_{DG}$ given by

$$\|\!|(\mathbf{v}, q)|\!\|_{DG}^2 = \nu\|\nabla_h \mathbf{v}\|_{0,\Omega}^2 + \nu\int_\mathcal{E} \mathtt{h}^{-1}|\underline{[\![\mathbf{v}]\!]}|^2\,ds + \nu^{-1}\|q\|_{0,\Omega}^2.$$

The following theorem is the main result of this paper.

THEOREM 3.1. *Let* $(\mathbf{u}, p) \in H_0^1(\Omega)^2 \times L_0^2(\Omega)$ *be the analytical solution of the Stokes problem (1) and* $(\mathbf{u}_h, p_h) \in \mathbf{V}_h \times Q_h$ *its mixed DG approximation obtained by (3). Then, the following a posteriori error bound holds: there exists a positive constant* C*, independent of* ν *and the mesh size, such that*

$$\|\!|(\mathbf{u}-\mathbf{u}_h, p-p_h)|\!\|_{DG} \le C\Big(\sum_{K\in\mathcal{T}_h} \eta_K^2\Big)^{1/2},$$

where the elemental error indicator η_K *is given by*

$$\begin{aligned}\eta_K^2 &= \nu^{-1}h_K^2\|\mathbf{f}+\nu\Delta\mathbf{u}_h - \nabla p_h\|_{0,K}^2 + \nu\|\nabla\cdot\mathbf{u}_h\|_{0,K}^2 \\ &\quad + \nu^{-1}h_K\|[\![p_h]\!] - [\![\nu\nabla_h\mathbf{u}_h]\!]\|_{0,\partial K\setminus\Gamma}^2 + \nu h_K^{-1}\|\underline{[\![\mathbf{u}_h]\!]}\|_{0,\partial K}^2.\end{aligned}$$

REMARK 3.1. *Note that, for simplicity, the error in the approximation of the source term* $\mathbf{f}$ *is not taken into account explicitly in Theorem 3.1. However, this can be done straightforwardly by using the triangle inequality, giving rise to a standard data oscillation term. We point out that, in our numerical results below, the source terms* $\mathbf{f}$ *are always chosen in such a way that the error in the data approximation can be neglected.*

REMARK 3.2. *To incorporate the inhomogeneous boundary conditions* $\mathbf{u} = \mathbf{g}$ *on* Γ*, the error indicators* η_K *are simply modified with a corresponding modification of the jump indicators* $\nu h_K^{-1} \| \underline{[\![\mathbf{u}_h]\!]} \|_{0,\partial K}^2$ *on* $\partial K \cap \Gamma$*, neglecting again data oscillation terms accounting for the approximation of boundary data.*

The proof of Theorem 3.1 is carried out in the next section. In contrast to the approach of Becker *et al.* [4] and Houston *et al.* [14], which is based on employing a suitable Helmholtz decomposition of the error, together with the underlying conservation properties of the DG method, our analysis here relies on a non-consistent reformulation of the method by using lifting operators in the spirit of Arnold *et al.* [1], Perugia and Schötzau [17] and Schötzau *et al.* [18], and then exploiting the recent decomposition result for discontinuous spaces from Houston *et al.* [13].

4. Proof of Theorem 3.1

The aim of this section is to prove Theorem 3.1; to this end, we proceed in the following steps.

4.1. Perturbed Formulation

We begin by introducing a non-consistent reformulation of the variational problem (3), following the ideas used by Arnold *et al.* [1], Perugia and Schötzau [17] and Schötzau *et al.* [18] for the a priori error analysis of DG methods.

First, we define the space

$$\mathbf{V}(h) = H_0^1(\Omega)^2 + \mathbf{V}_h, \tag{5}$$

endowed with the broken energy norm

$$\|\mathbf{v}\|_{1,h}^2 = \|\nabla_h \mathbf{v}\|_{0,\Omega}^2 + \int_{\mathcal{E}} \mathtt{h}^{-1} |\underline{[\![\mathbf{v}]\!]}|^2 \, ds.$$

Next, by using the auxiliary space

$$\underline{\Sigma}_h = \{ \underline{\tau} \in L^2(\Omega)^{2\times 2} : \underline{\tau}|_K \in \mathcal{Q}^k(K)^{2\times 2}, K \in \mathcal{T}_h \},$$

we introduce the lifting operator $\underline{\mathcal{L}} : \mathbf{V}(h) \to \underline{\Sigma}_h$ by

$$\int_\Omega \underline{\mathcal{L}}(\mathbf{v}) : \underline{\tau} \, d\mathbf{x} = \int_{\mathcal{E}} \underline{[\![\mathbf{v}]\!]} : \{\!\{\underline{\tau}\}\!\} \, ds \qquad \forall \underline{\tau} \in \underline{\Sigma}_h.$$

In addition, we define $\mathcal{M} : \mathbf{V}(h) \to Q_h$ by

$$\int_\Omega \mathcal{M}(\mathbf{v}) q \, d\mathbf{x} = \int_\mathcal{E} [\![v]\!] \{\!\{q\}\!\} \, ds \qquad \forall q \in Q_h.$$

The above lifting operators have the following stability properties; see Perugia and Schötzau [17] or Schötzau *et al.* [18] for details.

LEMMA 4.1. *There exists a positive constant C, independent of the mesh size, such that*

$$\|\underline{\mathcal{L}}(\mathbf{v})\|_{0,\Omega}^2 \le C \int_\mathcal{E} \mathtt{h}^{-1} |\underline{[\![\mathbf{v}]\!]}|^2 \, ds, \qquad \|\mathcal{M}(\mathbf{v})\|_{0,\Omega}^2 \le C \int_\mathcal{E} \mathtt{h}^{-1} |\underline{[\![\mathbf{v}]\!]}|^2 \, ds,$$

for any $\mathbf{v} \in \mathbf{V}(h)$.

We are now ready to introduce the following perturbed forms on $\mathbf{V}(h) \times \mathbf{V}(h)$ and $\mathbf{V}(h) \times L^2(\Omega)$, respectively:

$$\begin{aligned}
\widetilde{A}_h(\mathbf{u}, \mathbf{v}) &= \nu \int_\Omega \nabla_h \mathbf{u} : \nabla_h \mathbf{v} \, d\mathbf{x} - \int_\Omega (\underline{\mathcal{L}}(\mathbf{u}) : \nu \nabla_h \mathbf{v} + \underline{\mathcal{L}}(\mathbf{v}) : \nu \nabla_h \mathbf{u}) \, d\mathbf{x} \\
&\quad + \nu \int_\mathcal{E} \mathtt{c} \underline{[\![\mathbf{u}]\!]} : \underline{[\![\mathbf{v}]\!]} \, ds, \\
\widetilde{B}_h(\mathbf{v}, q) &= -\int_\Omega q \, \nabla_h \cdot \mathbf{v} \, d\mathbf{x} + \int_\Omega \mathcal{M}(\mathbf{v}) q \, d\mathbf{x}.
\end{aligned}$$

With the above forms, we can rewrite problem (3) in the equivalent form: find $(\mathbf{u}_h, p_h) \in \mathbf{V}_h \times Q_h$ such that

$$\left\{ \begin{array}{lclcl} \widetilde{A}_h(\mathbf{u}_h, \mathbf{v}) & + & \widetilde{B}_h(\mathbf{v}, p_h) & = & \int_\Omega \mathbf{f} \cdot \mathbf{v} \, d\mathbf{x}, \\ -\widetilde{B}_h(\mathbf{u}_h, q) & & & = & 0 \end{array} \right. \tag{6}$$

for all $(\mathbf{v}, q) \in \mathbf{V}_h \times Q_h$.

Then, by setting

$$\mathcal{A}_h(\mathbf{u}, p; \mathbf{v}, q) = \widetilde{A}_h(\mathbf{u}, \mathbf{v}) + \widetilde{B}_h(\mathbf{v}, p) - \widetilde{B}_h(\mathbf{u}, q),$$

for any $(\mathbf{u}, p), (\mathbf{v}, q) \in \mathbf{V}(h) \times L^2(\Omega)$, we may reformulate problem (3) as follows: find $(\mathbf{u}_h, p_h) \in \mathbf{V}_h \times Q_h$ such that

$$\mathcal{A}_h(\mathbf{u}_h, p_h; \mathbf{v}, q) = \int_\Omega \mathbf{f} \cdot \mathbf{v} \, d\mathbf{x} \tag{7}$$

for all $(\mathbf{v}, q) \in \mathbf{V}_h \times Q_h$.

Finally, for the analytical solution $(\mathbf{u}, p)$ of the Stokes problem (1), we introduce the residual

$$\mathcal{R}_h(\mathbf{u}, p; \mathbf{v}, q) = \mathcal{A}_h(\mathbf{u}, p; \mathbf{v}, q) - \int_\Omega \mathbf{f} \cdot \mathbf{v} \, d\mathbf{x}, \qquad (\mathbf{v}, q) \in \mathbf{V}_h \times Q_h. \quad (8)$$

In view of the non-consistency of the perturbed formulation in (7), the error equation reads as follows:

$$\mathcal{A}_h(\mathbf{u} - \mathbf{u}_h, p - p_h; \mathbf{v}, q) = \mathcal{R}_h(\mathbf{u}, p; \mathbf{v}, q), \qquad (\mathbf{v}, q) \in \mathbf{V}_h \times Q_h. \quad (9)$$

4.2. Stability Results

In this section, we collect some basic stability properties of the form $\mathcal{A}_h$. First of all, we have the following continuity result:

LEMMA 4.2. *There exists a positive constant C, independent of ν and the mesh size, such that*

$$|\mathcal{A}_h(\mathbf{u}, p; \mathbf{v}, q)| \leq C \|\!|(\mathbf{u}, p)|\!\|_{DG} \|\!|(\mathbf{v}, q)|\!\|_{DG},$$

for any $(\mathbf{u}, p), (\mathbf{v}, q) \in \mathbf{V}(h) \times L^2(\Omega)$.

Proof. This follows readily from the stability estimates for $\underline{\mathcal{L}}$ and $\mathcal{M}$ in Lemma 4.1, the definition of c and the forms $\widetilde{A}_h$ and $\widetilde{B}_h$, and the Cauchy-Schwarz inequality; see Schötzau *et al.* [18] for details. □

Next, we recall the following stability result for the form $\mathcal{A}_h$ restricted to $H_0^1(\Omega)^2 \times L_0^2(\Omega)$. This result is a direct consequence of the definition of the perturbed forms and the inf-sup condition in (2).

LEMMA 4.3. *There exists a positive constant C, independent of ν and the mesh size, such that for any $(\mathbf{u}, p) \in H_0^1(\Omega)^2 \times L_0^2(\Omega)$, there is $(\mathbf{v}, q) \in H_0^1(\Omega)^2 \times L_0^2(\Omega)$ with*

$$\mathcal{A}_h(\mathbf{u}, p; \mathbf{v}, q) \geq \|\!|(\mathbf{u}, p)|\!\|_{DG}^2, \qquad \|\!|(\mathbf{v}, q)|\!\|_{DG} \leq C \|\!|(\mathbf{u}, p)|\!\|_{DG}.$$

Proof. Let $p \in L_0^2(\Omega)$. Then, referring to (2) there exists $\mathbf{w} \in H_0^1(\Omega)^2$ such that

$$-\int_\Omega p \nabla \cdot \mathbf{w} \, d\mathbf{x} \geq \kappa \|p\|_{0,\Omega}^2, \qquad \|\mathbf{w}\|_{1,h} \leq \|p\|_{0,\Omega}. \quad (10)$$

Now, we choose

$$\mathbf{v} = \alpha \mathbf{u} + \nu^{-1} \beta \mathbf{w}, \qquad q = \alpha p,$$

with

$$\alpha = 1 + \kappa^{-2}, \qquad \beta = 2\kappa^{-1}.$$

Since $\mathbf{u}$ and $\mathbf{v}$ are in $H_0^1(\Omega)^2$, we have that $\underline{\mathcal{L}}(\mathbf{u}) = \underline{\mathcal{L}}(\mathbf{v}) = \underline{0}$, $\mathcal{M}(\mathbf{u}) = \mathcal{M}(\mathbf{v}) = 0$, together with $\underline{[\![\mathbf{u}]\!]} = \underline{[\![\mathbf{v}]\!]} = \underline{0}$ on $\mathcal{E}$. Hence, using the bounds in (10) and the arithmetic-geometric mean inequality, we obtain

$$\begin{aligned}
\mathcal{A}_h(\mathbf{u}, p; \mathbf{v}, q) &= \nu \int_\Omega \nabla \mathbf{u} : \nabla \mathbf{v} \, d\mathbf{x} - \int_\Omega p \nabla \cdot \mathbf{v} \, d\mathbf{x} + \int_\Omega q \nabla \cdot \mathbf{u} \, d\mathbf{x} \\
&= \nu\alpha \|\mathbf{u}\|_{1,h}^2 + \beta \int_\Omega \nabla \mathbf{u} : \nabla \mathbf{w} \, d\mathbf{x} - \nu^{-1}\beta \int_\Omega p \nabla \cdot \mathbf{w} \, d\mathbf{x} \\
&\geq \left(\nu\alpha - \frac{\nu\beta}{2\kappa}\right) \|\mathbf{u}\|_{1,h}^2 - \frac{\beta\nu^{-1}\kappa}{2} \|\mathbf{w}\|_{1,h}^2 + \beta\nu^{-1}\kappa \|p\|_{0,\Omega}^2 \\
&\geq \left(\alpha - \frac{\beta\kappa^{-1}}{2}\right) \nu \|\mathbf{u}\|_{1,h}^2 + \frac{1}{2}\beta\nu^{-1}\kappa \|p\|_{0,\Omega}^2 \\
&= |\!|\!| (\mathbf{u}, p) |\!|\!|_{DG}^2.
\end{aligned}$$

Furthermore, employing the triangle inequality, we get

$$\begin{aligned}
|\!|\!| (\mathbf{v}, q) |\!|\!|_{DG}^2 &= \nu \|\mathbf{v}\|_{1,h}^2 + \nu^{-1} \|q\|_{0,\Omega}^2 \\
&\leq 2\nu\alpha^2 \|\mathbf{u}\|_{1,h}^2 + 2\nu^{-1}\beta^2 \|\mathbf{w}\|_{1,h}^2 + \nu^{-1}\alpha^2 \|p\|_{0,\Omega}^2 \\
&\leq 2\nu\alpha^2 \|\mathbf{u}\|_{1,h}^2 + (2\beta^2 + \alpha^2)\nu^{-1} \|p\|_{0,\Omega}^2 \\
&\leq C |\!|\!| (\mathbf{u}, p) |\!|\!|_{DG}^2,
\end{aligned}$$

which completes the proof. □

Finally, we state a decomposition result for discontinuous finite element spaces. To this end, let $\mathbf{V}_h^c = \mathbf{V}_h \cap H_0^1(\Omega)^2$. The orthogonal complement in $\mathbf{V}$ of $\mathbf{V}_h^c$ with respect to the norm $\|\cdot\|_{1,h}$ is denoted by $\mathbf{V}_h^\perp$. Under the foregoing assumptions on the meshes, the following equivalence result holds. The proof can be found in Houston *et al.* [13]; it crucially relies on an approximation result of Karakashian and Pascal [16, Section 2.1].

PROPOSITION 4.1. *The expression*

$$\mathbf{v} \mapsto \left(\int_{\mathcal{E}} \mathtt{h}^{-1} |\underline{[\![\mathbf{v}]\!]}|^2 \, ds \right)^{\frac{1}{2}}$$

is a norm on $\mathbf{V}_h^\perp$ *that is equivalent to the norm* $\|\cdot\|_{1,h}$*, with equivalence constants that are independent of the mesh size.*

4.3. An Auxiliary Result

Next, we prove an auxiliary result. To this end, we let $(\mathbf{v}, q) \in H_0^1(\Omega)^2 \times L_0^2(\Omega)$ be arbitrary; further, we write $(\mathbf{v}_h, q_h) \in \mathbf{V}_h \times Q_h$ to denote an approximation to $(\mathbf{v}, q)$ satisfying

$$\sum_{K\in\mathcal{T}_h} (h_K^{-2}\|\mathbf{v}-\mathbf{v}_h\|_{0,K}^2+\|\nabla(\mathbf{v}-\mathbf{v}_h)\|_{0,K}^2+h_K^{-1}\|\mathbf{v}-\mathbf{v}_h\|_{0,\partial K}^2) \leq C\|\nabla\mathbf{v}\|_{0,\Omega}^2, \tag{11}$$

as well as,

$$\|q - q_h\|_{0,\Omega} \leq C\|q\|_{0,\Omega}. \tag{12}$$

These assumptions are satisfied, for example, if $\mathbf{v}_h$ and q_h are chosen to be L^2-projections of $\mathbf{v}$ and q onto $\mathbf{V}_h$ and Q_h, respectively.

With this notation, we have the following result.

PROPOSITION 4.2. *Under the foregoing assumptions (11) and (12), the following inequality holds*

$$\left|\int_\Omega \mathbf{f}\cdot(\mathbf{v}-\mathbf{v}_h)\,d\mathbf{x} - \mathcal{A}_h(\mathbf{u}_h, p_h; \mathbf{v}-\mathbf{v}_h, q-q_h)\right| \leq C\Big(\sum_{K\in\mathcal{T}_h}\eta_K^2\Big)^{\frac{1}{2}} |||(\mathbf{v}, q)|||_{DG},$$

where C is a positive constant, independent of ν and the mesh size.

Proof. We set $\xi_{\mathbf{v}} = \mathbf{v} - \mathbf{v}_h$, $\xi_q = q - q_h$, and

$$T = \int_\Omega \mathbf{f}\cdot\xi_{\mathbf{v}}\,d\mathbf{x} - \mathcal{A}_h(\mathbf{u}_h, p_h; \xi_{\mathbf{v}}, \xi_q).$$

We first note that

$$T = \int_\Omega \mathbf{f}\cdot\xi_{\mathbf{v}}\,d\mathbf{x} - \widetilde{A}_h(\mathbf{u}_h, \xi_{\mathbf{v}}) - \widetilde{B}_h(\xi_{\mathbf{v}}, p_h) + \widetilde{B}_h(\mathbf{u}_h, \xi_q). \tag{13}$$

Integration by parts and the definition of the lifting operator $\underline{\mathcal{L}}$ leads to

$$\begin{aligned} -\widetilde{A}_h(\mathbf{u}_h, \xi_{\mathbf{v}}) \;=\; & \sum_{K\in\mathcal{T}_h}\left(\int_K \nu\Delta\mathbf{u}_h\cdot\xi_{\mathbf{v}}\,d\mathbf{x} - \int_{\partial K}\nu\nabla_h\mathbf{u}_h : (\xi_{\mathbf{v}}\otimes\mathbf{n}_K)ds\right) \\ & + \int_\Omega \nu\underline{\mathcal{L}}(\mathbf{u}_h) : \nabla_h\xi_{\mathbf{v}}\,d\mathbf{x} + \int_\Omega \nu\underline{\mathcal{L}}(\xi_{\mathbf{v}}) : \nabla_h\mathbf{u}_h\,d\mathbf{x} \\ & -\nu\int_{\mathcal{E}} \mathtt{c}\underline{[\![\mathbf{u}_h]\!]} : \underline{[\![\xi_{\mathbf{v}}]\!]}\,ds \end{aligned}$$

$$= \sum_{K\in\mathcal{T}_h} \int_K \nu\Delta\mathbf{u}_h\cdot\xi_{\mathbf{v}}\,d\mathbf{x} - \int_{\mathcal{E}_\mathcal{I}} [\![\nu\nabla_h\mathbf{u}_h]\!]\cdot\{\!\{\xi_{\mathbf{v}}\}\!\}\,ds$$
$$+ \int_\Omega \nu\mathcal{L}(\mathbf{u}_h):\nabla_h\xi_{\mathbf{v}}\,d\mathbf{x} - \nu\int_{\mathcal{E}} \mathsf{c}\underline{[\![\mathbf{u}_h]\!]}:\underline{[\![\xi_{\mathbf{v}}]\!]}\,ds.$$

Similarly, by integration by parts, we obtain

$$-\widetilde{B}_h(\xi_{\mathbf{v}},p_h)+\widetilde{B}_h(\mathbf{u}_h,\xi_q) = -\sum_{K\in\mathcal{T}_h}\int_K \nabla p_h\cdot\xi_{\mathbf{v}}\,d\mathbf{x} + \int_{\mathcal{E}_\mathcal{I}} [\![p_h]\!]\cdot\{\!\{\xi_{\mathbf{v}}\}\!\}\,ds$$
$$-\sum_{K\in\mathcal{T}_h}\int_K \xi_q\nabla\cdot\mathbf{u}_h\,d\mathbf{x} + \int_\Omega \mathcal{M}(\mathbf{u}_h)\xi_q\,d\mathbf{x}.$$

Substituting the above expressions into (13), we get

$$\begin{aligned} T \;=\; & \sum_{K\in\mathcal{T}_h}\int_K (\mathbf{f}+\nu\Delta\mathbf{u}_h-\nabla p_h)\cdot\xi_{\mathbf{v}}\,d\mathbf{x} - \sum_{K\in\mathcal{T}_h}\int_K \xi_q\nabla_h\cdot\mathbf{u}_h\,d\mathbf{x} \\ & + \int_{\mathcal{E}_\mathcal{I}} ([\![p_h]\!]-[\![\nu\nabla_h\mathbf{u}_h]\!])\cdot\{\!\{\xi_{\mathbf{v}}\}\!\}\,ds - \nu\int_{\mathcal{E}} \mathsf{c}\underline{[\![\mathbf{u}_h]\!]}:\underline{[\![\xi_{\mathbf{v}}]\!]}\,ds \\ & + \int_\Omega \nu\mathcal{L}(\mathbf{u}_h):\nabla_h\xi_{\mathbf{v}}\,d\mathbf{x} + \int_\Omega \mathcal{M}(\mathbf{u}_h)\xi_q\,d\mathbf{x}. \end{aligned}$$

Using the weighted Cauchy-Schwarz inequality, the stability bounds from Lemma 4.1, and noting that $|[\![\mathbf{u}_h]\!]|\le|\underline{[\![\mathbf{u}_h]\!]}|$, we conclude that

$$\begin{aligned} |T| \le C\Big(\sum_{K\in\mathcal{T}_h}\eta_K^2\Big)^{\frac12} & \\ \times\Big(\sum_{K\in\mathcal{T}_h} \nu h_K^{-2}\|\xi_{\mathbf{v}}\|_{0,K}^2+\nu\|\nabla\xi_{\mathbf{v}}\|_{0,K}^2+\nu h_K^{-1}\|\xi_{\mathbf{v}}\|_{0,\partial K}^2+\nu^{-1}\|\xi_q\|_{0,K}^2\Big)^{\frac12}. \end{aligned}$$

The application of (11) and (12) completes the proof. $\square$

4.4. A Posteriori Error Estimation

In this section we complete the proof of Theorem 3.1. To this end, we denote the error of the DG approximation by $(\mathbf{e}_u,e_p)=(\mathbf{u}-\mathbf{u}_h,p-p_h)$. Furthermore, we decompose $\mathbf{u}_h$ into $\mathbf{u}_h=\mathbf{u}_h^c\oplus\mathbf{u}_h^\perp$, in accordance with the decomposition in Section 4.2 and Proposition 4.1. We then set $\mathbf{e}_u^c=\mathbf{u}-\mathbf{u}_h^c$.

Using the equivalence result in Proposition 4.1 and the fact that $\underline{[\![\mathbf{u}_h]\!]}=\underline{[\![\mathbf{u}_h^\perp]\!]}$, we have

$$|\!|\!|(\mathbf{e}_u,e_p)|\!|\!|_{DG}^2 \;\le\; C\left(|\!|\!|(\mathbf{e}_u^c,e_p)|\!|\!|_{DG}^2+\nu\|\mathbf{u}_h^\perp\|_{1,h}^2\right)$$

$$\leq C\left(\|(\mathbf{e}_u^c, e_p)\|_{DG}^2 + \nu \int_{\mathcal{E}} \mathtt{h}^{-1} |\underline{[\![\mathbf{u}_h]\!]}|^2 \, ds\right)$$
$$\leq C\left(\|(\mathbf{e}_u^c, e_p)\|_{DG}^2 + \sum_{K\in\mathcal{T}_h} \eta_K^2\right).$$

To bound the term $\|(\mathbf{e}_u^c, e_p)\|_{DG}^2$, we invoke the stability result from Lemma 4.3 and obtain a function $(\mathbf{v}, q) \in H_0^1(\Omega)^2 \times L_0^2(\Omega)$ such that

$$\|(\mathbf{e}_u^c, e_p)\|_{DG}^2 \leq \mathcal{A}_h(\mathbf{e}_u^c, e_p; \mathbf{v}, q), \qquad \|(\mathbf{v}, q)\|_{DG} \leq C\|(\mathbf{e}_u^c, e_p)\|_{DG}. \tag{14}$$

Let $(\mathbf{v}_h, q_h) \in \mathbf{V}_h \times Q_h$ be arbitrary. Elementary manipulations, combined with the error equation (9), lead to

$$\begin{aligned}
\|(\mathbf{e}_u^c, e_p)\|_{DG}^2 &\leq \mathcal{A}_h(\mathbf{e}_u^c, e_p; \mathbf{v}, q) \\
&= \mathcal{A}_h(\mathbf{e}_u, e_p; \mathbf{v}, q) + \mathcal{A}_h(\mathbf{u}_h^\perp, 0; \mathbf{v}, q) \\
&= \mathcal{A}_h(\mathbf{e}_u, e_p; \mathbf{v} - \mathbf{v}_h, q - q_h) + \mathcal{R}_h(\mathbf{u}, p; \mathbf{v}_h, q_h) \\
&\quad + \mathcal{A}_h(\mathbf{u}_h^\perp, 0; \mathbf{v}, q) \\
&= \mathcal{A}_h(\mathbf{u}, p; \mathbf{v} - \mathbf{v}_h, q - q_h) - \mathcal{A}_h(\mathbf{u}_h, p_h; \mathbf{v} - \mathbf{v}_h, q - q_h) \\
&\quad + \mathcal{R}_h(\mathbf{u}, p; \mathbf{v}_h, q_h) + \mathcal{A}_h(\mathbf{u}_h^\perp, 0; \mathbf{v}, q).
\end{aligned}$$

Since $(\mathbf{v}, q) \in H_0^1(\Omega)^2 \times L_0^2(\Omega)$, we note that, with the definition (8) of the residual and the weak formulation of the Stokes problem,

$$\begin{aligned}
\mathcal{A}_h(\mathbf{u}, p; \mathbf{v} - \mathbf{v}_h, q - q_h) &= \mathcal{A}_h(\mathbf{u}, p; \mathbf{v}, q) - \mathcal{A}_h(\mathbf{u}, p; \mathbf{v}_h, q_h) \\
&= \int_\Omega \mathbf{f} \cdot (\mathbf{v} - \mathbf{v}_h) \, d\mathbf{x} - \mathcal{R}_h(\mathbf{u}, p; \mathbf{v}_h, q_h).
\end{aligned}$$

This yields

$$\begin{aligned}
\|(\mathbf{e}_u^c, e_p)\|_{DG}^2 &\leq |\mathcal{A}_h(\mathbf{u}_h^\perp, 0; \mathbf{v}, q)| \\
&\quad + \left|\int_\Omega \mathbf{f} \cdot (\mathbf{v} - \mathbf{v}_h) \, d\mathbf{x} - \mathcal{A}_h(\mathbf{u}_h, p_h; \mathbf{v} - \mathbf{v}_h, q - q_h)\right| \\
&\leq C\left(\sum_{K\in\mathcal{T}_h} \eta_K^2\right)^{\frac{1}{2}} \|(\mathbf{v}, q)\|_{DG}.
\end{aligned}$$

Here, we have used the continuity of $\mathcal{A}_h$ from Lemma 4.2, the equivalence result from Proposition 4.1 and the auxiliary result from Proposition 4.2. Using the bound (14) for $(\mathbf{v}, q)$ gives

$$\|(\mathbf{e}_u^c, e_p)\|_{DG}^2 \leq C \sum_{K\in\mathcal{T}_h} \eta_K^2,$$

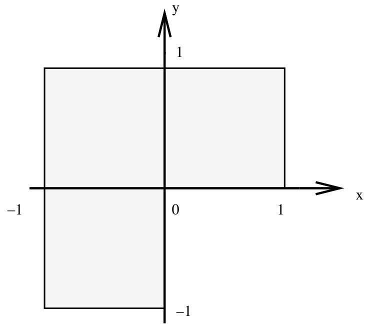

Figure 1. L–shaped domain Ω.

which completes the proof of Theorem 3.1.

5. Numerical Experiments

In this section we present a series of numerical examples to illustrate the practical performance of the proposed a posteriori error estimator within an automatic adaptive refinement procedure. In each of the examples shown below, we set the polynomial degree k equal to 1 and the constant γ arising in the definition of the interior penalty parameter $\mathtt{c}$, cf. (4), equal to 10. The adaptive meshes are constructed by employing the fixed fraction strategy, with refinement and derefinement fractions set to 25% and 10%, respectively. Here, the emphasis will be to demonstrate the asymptotic exactness of the proposed a posteriori error indicator on non-uniform adaptively refined meshes. Thereby, as in Becker *et al.* [3], we set the constant C arising in Theorem 3.1 equal to one and ensure that the corresponding effectivity indices are roughly constant on all of the meshes employed; in general, to ensure the reliability of the error estimator, C must be numerically determined for the underlying problem at hand, cf. Eriksson *et al.* [9], for example.

5.1. Example 1

Here, we let Ω be the L–shaped domain shown in Figure 1; further, we select $\nu = 1$, $\mathbf{f} = \mathbf{0}$ and enforce appropriate inhomogeneous boundary conditions for $\mathbf{u}$ on Γ so that the analytical solution to (1) is given by

$$\begin{pmatrix} \mathbf{u}_1 \\ \mathbf{u}_2 \\ p \end{pmatrix} = \begin{pmatrix} -\mathrm{e}^x(y\cos(y) + \sin(y)) \\ \mathrm{e}^x y \sin(y) \\ 2\mathrm{e}^x \sin(y) - (2(1-\mathrm{e})(\cos(1)-1))/3 \end{pmatrix}.$$

In Figure 2(a) we show the mesh generated using the proposed a posteriori error indicator after 10 adaptive refinement steps. Here, we see that

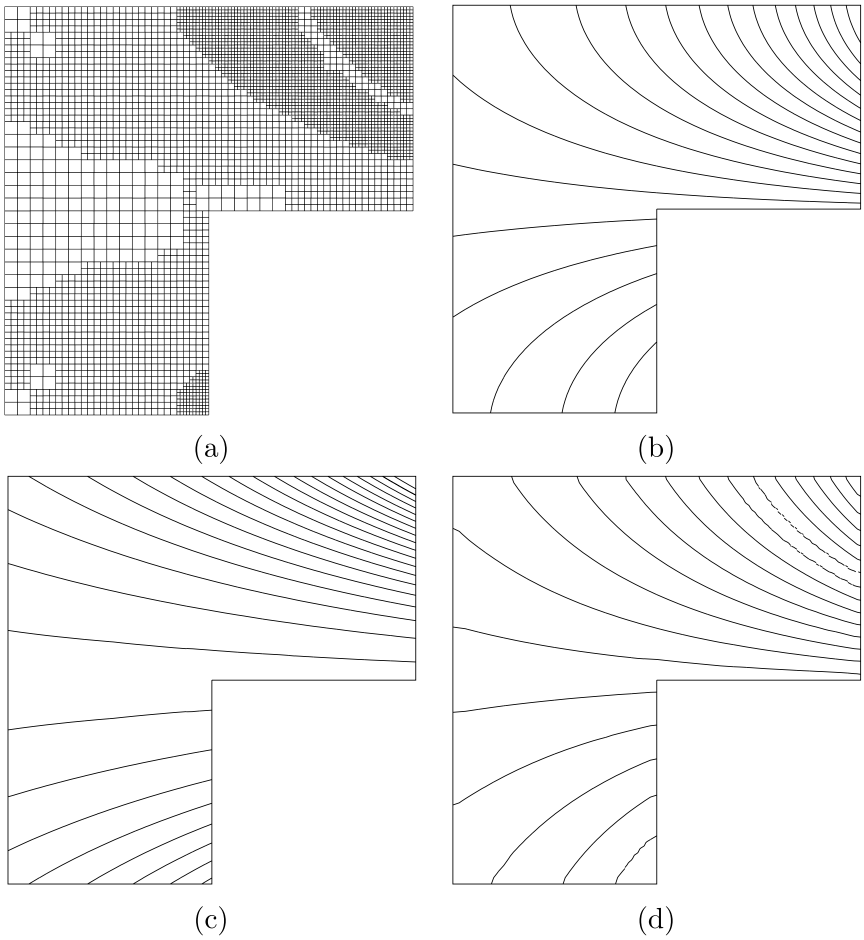

Figure 2. Example 1. (a) Computational mesh with 4359 elements, after 10 adaptive refinements. Numerical approximation to: (b) $\mathbf{u}_1$; (c) $\mathbf{u}_2$; (d) p.

while the mesh has been largely uniformly refined throughout the entire computational domain, additional refinement has been performed where the gradient/curvature of the analytical solution is relativity large; cf. Figures 2(b), (c) and (d), where we plot the isolines of the numerical approximation to $\mathbf{u}_1$, $\mathbf{u}_2$ and p, respectively, computed on this mesh.

Finally, in Figure 3(a) we present a comparison of the actual and estimated energy norm of the error, versus the number of degrees of freedom in the finite element space $\mathbf{V}_h \times Q_h$, on the sequence of meshes generated by our adaptive algorithm. Here, we observe that the error bound over-estimates the true error by a consistent factor; indeed, from

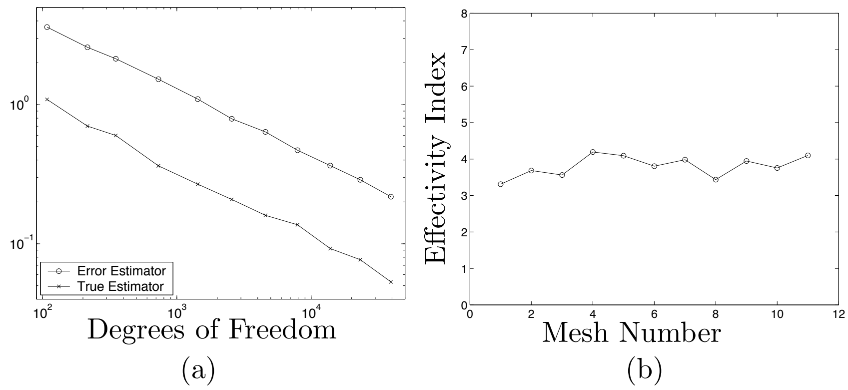

Figure 3. Example 1. (a) Comparison of the actual and estimated energy norm of the error with respect to the number of degrees of freedom; (b) Effectivity Indices.

Figure 3(b), we see that the computed effectivity indices lie in the range between 3–4, thereby confirming the asymptotic exactness of the proposed error indicator for this smooth problem.

5.2. Example 2

In this section, we consider the example of the singular solution to (1) proposed in Verfürth [21, p. 113]. To this end, we again let Ω be the L–shaped domain shown in Figure 1, and select $\mathbf{f} = \mathbf{0}$ and $\nu = 1$. Then, writing (r, φ) to denote the system of polar coordinates, we impose an appropriate inhomogeneous boundary condition for $\mathbf{u}$ so that

$$\begin{aligned} \mathbf{u}(r,\varphi) &= r^{\lambda} \begin{pmatrix} (1+\lambda)\sin(\varphi)\Psi(\varphi) + \cos(\varphi)\Psi'(\varphi) \\ \sin(\varphi)\Psi'(\varphi) - (1+\lambda)\cos(\varphi)\Psi(\varphi) \end{pmatrix}, \\ p &= -r^{\lambda-1}[(1+\lambda)^2\Psi'(\varphi) + \Psi'''(\varphi)]/(1-\lambda), \end{aligned}$$

where

$$\begin{aligned} \Psi(\varphi) &= \sin((1+\lambda)\varphi)\cos(\lambda\omega)/(1+\lambda) - \cos((1+\lambda)\varphi) \\ &\quad - \sin((1-\lambda)\varphi)\cos(\lambda\omega)/(1-\lambda) + \cos((1-\lambda)\varphi), \\ \omega &= \frac{3\pi}{2}. \end{aligned}$$

The exponent λ is the smallest positive solution of

$$\sin(\lambda\omega) + \lambda\sin(\omega) = 0;$$

thereby, $\lambda \approx 0.54448373678246$.

We emphasize that $(\mathbf{u}, p)$ is analytic in $\overline{\Omega} \setminus \{\mathbf{0}\}$, but both $\nabla\mathbf{u}$ and p are singular at the origin; indeed, here $\mathbf{u} \notin H^2(\Omega)^2$ and $p \notin H^1(\Omega)$.

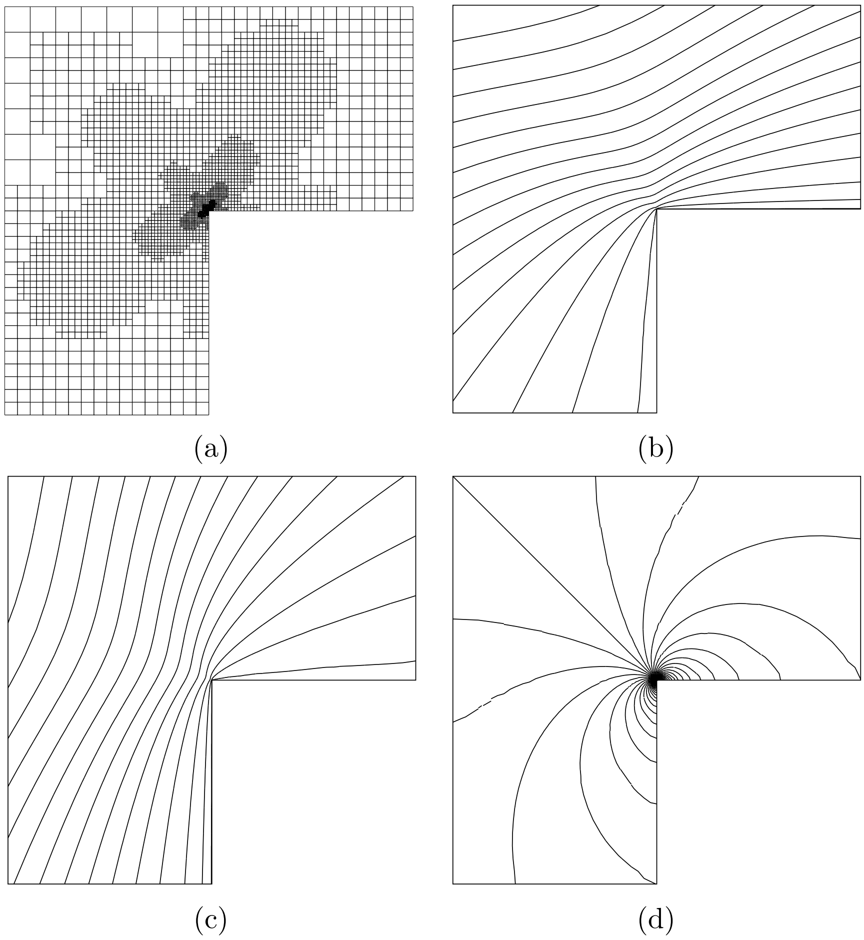
(a) (b) (c) (d)

Figure 4. Example 2. (a) Computational mesh with 3009 elements, after 8 adaptive refinements. Numerical approximation to: (b) $\mathbf{u}_1$; (c) $\mathbf{u}_2$; (d) p.

This example reflects the typical (singular) behavior that solutions of the Stokes problem exhibit in the vicinity of reentrant corners in the computational domain.

In Figure 4(a) we show the mesh generated using the local error indicators η_K after 8 adaptive refinement steps. Here, we see that the mesh has been largely refined in the vicinity of the re-entrant corner located at the origin, as well as in the region adjacent to this singular point; indeed, away from the origin, we see that the mesh is (almost) symmetric about the line $y = -x$. The isolines of the numerical approximation $(\mathbf{u}_h, p_h)$ computed on this mesh are shown in Figures 4(b), (c) and (d), respectively. Finally, Figure 5 shows the history of the actual

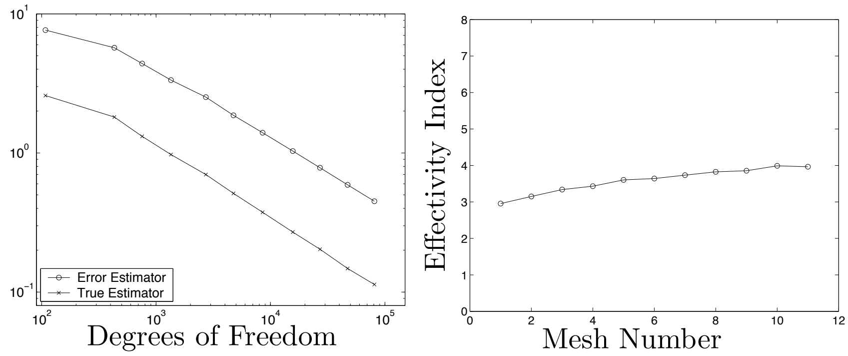

(a) (b)

Figure 5. Example 2. (a) Comparison of the actual and estimated energy norm of the error with respect to the number of degrees of freedom; (b) Effectivity Indices.

and estimated energy norm of the error on each of the meshes generated by our adaptive algorithm, together with their corresponding effectivity indices. As in the previous example, we observe that the a posteriori bound over-estimates the true error by a consistent factor between 3–4, though here we do see that for this non-smooth example, the effectivity indices do grow very slightly as the mesh is refined; asymptotically they seem to be tending towards a constant value of approximately 4, thereby confirming the asymptotic exactness of the error indicator.

6. Concluding Remarks

In this paper, we have derived a residual–based energy norm a posteriori error bound for mixed DG approximations of the Stokes equations. The analysis is based on employing a non-consistent reformulation of the DG scheme, together with a decomposition result for the underlying discontinuous space. Numerical experiments presented in this article clearly highlight the asymptotic exactness of the proposed estimator on adaptively refined meshes. Future work will be devoted to the extension of our analysis to *hp*-adaptive discontinuous Galerkin approximations of more complicated incompressible flow models.

References

1. D.N. Arnold, F. Brezzi, B. Cockburn, and L.D. Marini. Unified analysis of discontinuous Galerkin methods for elliptic problems. *SIAM J. Numer. Anal.*, 39:1749–1779, 2001.

2. G.A. Baker, W.N. Jureidini, and O.A. Karakashian. Piecewise solenoidal vector fields and the Stokes problem. *SIAM J. Numer. Anal.*, 27:1466–1485, 1990.
3. R. Becker, P. Hansbo, and M.G. Larson. Energy norm a posteriori error estimation for discontinuous Galerkin methods. *Comput. Methods Appl. Mech. Engrg.*, 192:723–733, 2003.
4. R. Becker, P. Hansbo, and R. Stenberg. A finite element method for domain decomposition with non-matching grids. *Modél. Math. Anal. Numér.*, 37:209–225, 2003.
5. F. Brezzi and M. Fortin. Mixed and hybrid finite element methods. In *Springer Series in Computational Mathematics*, volume 15. Springer–Verlag, New York, 1991.
6. B. Cockburn, G. Kanschat, and D. Schötzau. The local discontinuous Galerkin method for the Oseen equations. Technical Report 02-05, Department of Mathematics, University of Basel, 2002. In press in Math. Comp.
7. B. Cockburn, G. Kanschat, D. Schötzau, and C. Schwab. Local discontinuous Galerkin methods for the Stokes system. *SIAM J. Numer. Anal.*, 40:319–343, 2002.
8. M. Dauge. Stationary Stokes and Navier–Stokes systems on two- or three-dimensional domains with corners. Part I: Linearized equations. *SIAM J. Math. Anal.*, 20(1):74–97, 1989.
9. K. Eriksson, D. Estep, P. Hansbo, and C. Johnson. Introduction to adaptive methods for differential equations. In A. Iserles, editor, *Acta Numerica*, pages 105–158. Cambridge University Press, 1995.
10. V. Girault and P.A. Raviart. *Finite element methods for Navier–Stokes equations*. Springer–Verlag, New York, 1986.
11. V. Girault, B. Rivière, and M.F. Wheeler. A discontinuous Galerkin method with non-overlapping domain decomposition for the Stokes and Navier-Stokes problems. Technical Report 02-08, TICAM, UT Austin, 2002.
12. P. Hansbo and M.G. Larson. Discontinuous finite element methods for incompressible and nearly incompressible elasticity by use of Nitsche's method. *Comput. Methods Appl. Mech. Engrg.*, 191:1895–1908, 2002.
13. P. Houston, I. Perugia, and D. Schötzau. Mixed discontinuous Galerkin approximation of the Maxwell operator. Technical Report 02-16, University of Basel, Department of Mathematics, 2002.
14. P. Houston, I. Perugia, and D. Schötzau. Energy norm *a posteriori* error estimation for mixed discontinuous Galerkin approximations of the Maxwell operator. *Submitted for publication*, 2003.
15. O.A. Karakashian and W.N. Jureidini. A nonconforming finite element method for the stationary Navier-Stokes equations. *SIAM J. Numer. Anal.*, 35:93–120, 1998.
16. O.A. Karakashian and F. Pascal. A posteriori error estimation for a discontinuous Galerkin approximation of second order elliptic problems. Technical report, University of Tennessee, Department of Mathematics, 2003. URL: `http://www.math.utk.edu/~ ohannes/papers.html`.
17. I. Perugia and D. Schötzau. An *hp*-analysis of the local discontinuous Galerkin method for diffusion problems. *J. Sci. Comput.*, 17:561–571, 2002.
18. D. Schötzau, C. Schwab, and A. Toselli. Mixed *hp*-DGFEM for incompressible flows. *SIAM J. Numer. Anal.*, 40:2171–2194, 2003.
19. D. Schötzau and T.P. Wihler. Exponential convergence of mixed *hp*-DGFEM for Stokes flow in polygons. Technical Report 2002-15, Department of Mathematics, University of Basel, 2002. In press in Numer. Math.

20. A. Toselli. *hp*-Discontinuous Galerkin approximations for the Stokes problem. *Math. Models Methods Appl. Sci.*, 12:1565–1616, 2002.
21. R. Verfürth. *A Review of a Posteriori Error Estimation and Adaptive Mesh-Refinement Techniques*. B.G. Teubner, Stuttgart, 1996.
22. T.P. Wihler, P. Frauenfelder, and C. Schwab. Exponential convergence of the *hp*-DGFEM for diffusion problems. *Comput. Math. Appl.*, 2003. To appear.

Research Reports

No.	Authors	Title
03-09	P. Houston, D. Schötzau, Th. Wihler	Energy norm a-posteriori error estimation for mixed discontinuous Galerkin approximations of the Stokes problem
03-08	R. Hiptmair, A. Buffa	Coercive combined field integral equations
03-07	R. Hiptmair, O. Sterz	Current and Voltage Excitations for the Eddy Current Model
03-06	A.-M. Matache, P.-A. Nitsche, C. Schwab	Wavelet Galerkin Pricing of American Options on Lévy Driven Assets
03-05	M. Becheanu, R.A. Todor	On the Set of Diameters of Finite Point-Sets in the Plane
03-04	C. Schwab, R.A. Todor	Sparse finite elements for stochastic elliptic problems - higher order moments
03-03	R. Sperb	Bounds for the first eigenvalue of the elastically supported membrane on convex domains
03-02	F.M. Buchmann	Computing exit times with the Euler scheme
03-01	A. Toselli, X. Vasseur	Domain decomposition preconditioners of Neumann-Neumann type for *hp*-approximations on boundary layer meshes in three dimensions
02-26	M. Savelieva	Theoretical study of axisymmetrical triple flame
02-25	D. Schötzau, C. Schwab, A. Toselli	Mixed *hp*-DGFEM for incompressible flows III: Pressure stabilization
02-24	F.M. Buchmann, W.P. Petersen	A stochastically generated preconditioner for stable matrices
02-23	A.W. Rüegg, A. Schneebeli, R. Lauper	Generalized *hp*-FEM for Lattice Structures
02-22	L. Filippini, A. Toselli	*hp* Finite Element Approximations on Non-Matching Grids for the Stokes Problem
02-21	D. Schötzau, C. Schwab, A. Toselli	Mixed *hp*-DGFEM for incompressible flows II: Geometric edge meshes
02-20	A. Toselli, X. Vasseur	A numerical study on Neumann-Neumann and FETI methods for *hp*-approximations on geometrically refined boundary layer meshes in two dimensions
02-19	D. Schötzau, Th.P. Wihler	Exponential convergence of mixed *hp*-DGFEM for Stokes flow in polygons
02-18	P.-A. Nitsche	Sparse approximation of singularity functions